



Article

# S-Acetyl-Glutathione Attenuates Carbon Tetrachloride-Induced Liver Injury by Modulating Oxidative Imbalance and Inflammation

Rosanna Di Paola <sup>1,†</sup> , Sergio Modafferi <sup>2,†</sup>, Rosalba Siracusa <sup>3</sup> , Marika Cordaro <sup>4</sup> , Ramona D'Amico <sup>3</sup> , Maria Laura Ontario <sup>2</sup>, Livia Interdonato <sup>3</sup>, Angela Trovato Salinaro <sup>2,\*</sup> , Roberta Fusco <sup>5,\*</sup> , Daniela Impellizzeri <sup>3</sup> , Vittorio Calabrese <sup>2,‡</sup> and Salvatore Cuzzocrea <sup>3,‡</sup>

- <sup>1</sup> Department of Veterinary Sciences, University of Messina, 98168 Messina, Italy; dipaolar@unime.it
  - <sup>2</sup> Department of Biomedical and Biotechnological Sciences, University of Catania, 95124 Catania, Italy; sergio.modafferi@studium.unict.it (S.M.); marialaura.ontario@ontariosrl.it (M.L.O.); calabres@unict.it (V.C.)
  - <sup>3</sup> Department of Chemical, Biological, Pharmaceutical and Environmental Sciences, University of Messina, Viale Ferdinando Stagno D'Alcontres 31, 98166 Messina, Italy; rsiracusa@unime.it (R.S.); rdamico@unime.it (R.D.); linterdonato@unime.it (L.I.); dimpellizzeri@unime.it (D.I.); salvator@unime.it (S.C.)
  - <sup>4</sup> Department of Biomedical, Dental and Morphological and Functional Imaging, University of Messina, Via Consolare Valeria, 98125 Messina, Italy; marika.cordaro@unime.it
  - <sup>5</sup> Department of Clinical and Experimental Medicine, University of Messina, Via Consolare Valeria, 98125 Messina, Italy
- \* Correspondence: trovato@unict.it (A.T.S.); rfusco@unime.it (R.F.)  
† These authors equally contributed to the work.  
‡ These authors contributed equally to this work.



**Citation:** Di Paola, R.; Modafferi, S.; Siracusa, R.; Cordaro, M.; D'Amico, R.; Ontario, M.L.; Interdonato, L.; Salinaro, A.T.; Fusco, R.; Impellizzeri, D.; et al. S-Acetyl-Glutathione Attenuates Carbon Tetrachloride-Induced Liver Injury by Modulating Oxidative Imbalance and Inflammation. *Int. J. Mol. Sci.* **2022**, *23*, 4429. <https://doi.org/10.3390/ijms23084429>

Academic Editor: Stefania Bruno

Received: 8 March 2022

Accepted: 15 April 2022

Published: 17 April 2022

**Publisher's Note:** MDPI stays neutral with regard to jurisdictional claims in published maps and institutional affiliations.



**Copyright:** © 2022 by the authors. Licensee MDPI, Basel, Switzerland. This article is an open access article distributed under the terms and conditions of the Creative Commons Attribution (CC BY) license (<https://creativecommons.org/licenses/by/4.0/>).

**Abstract:** Liver fibrosis, depending on the stage of the disease, could lead to organ dysfunction and cirrhosis, and no effective treatment is actually available. Emergent proof supports a link between oxidative stress, liver fibrogenesis and mitochondrial dysfunction as molecular bases of the pathology. A valid approach to protect against the disease would be to replenish the endogenous antioxidants; thus, we investigated the protective mechanisms of the S-acetyl-glutathione (SAG), a glutathione (GSH) prodrug. Preliminary in vitro analyses were conducted on primary hepatic cells. SAG pre-treatment significantly protected against cytotoxicity induced by CCl<sub>4</sub>. Additionally, CCl<sub>4</sub> induced a marked increase in AST and ALT levels, whereas SAG significantly reduced these levels, reaching values found in the control group. For the in vivo analyses, mice were administered twice a week with eight consecutive intraperitoneal injections of 1 mL/kg CCl<sub>4</sub> (diluted at 1:10 in olive oil) to induce oxidative imbalance and liver inflammation. SAG (30 mg/kg) was administered orally for 8 weeks. SAG significantly restored SOD activity, GSH levels and GPx activity, while it strongly reduced GSSG levels, lipid peroxidation and H<sub>2</sub>O<sub>2</sub> and ROS levels in the liver. Additionally, CCl<sub>4</sub> induced a decrease in anti-oxidants, including Nrf2, HO-1 and NQO-1, which were restored by treatment with SAG. The increased oxidative stress characteristic on liver disfunction causes the impairment of mitophagy and accumulation of dysfunctional and damaged mitochondria. Our results showed the protective effect of SAG administration in restoring mitophagy, as shown by the increased PINK1 and Parkin expressions in livers exposed to CCl<sub>4</sub> intoxication. Thus, the SAG administration showed anti-inflammatory effects decreasing pro-inflammatory cytokines TNF- $\alpha$ , IL-6, MCP-1 and IL-1 $\beta$  in both serum and liver, and suppressing the TLR4/NF $\kappa$ B pathway. SAG attenuated reduced fibrosis, collagen deposition, hepatocellular damage and organ dysfunction. In conclusion, our results suggest that SAG administration protects the liver from CCl<sub>4</sub> intoxication by restoring the oxidative balance, ameliorating the impairment of mitophagy and leading to reduced inflammation.

**Keywords:** liver fibrosis; antioxidant; inflammation

## 1. Introduction

Liver fibrosis is a characteristic result of chronic liver injury. It is caused by numerous insults, including toxic damage, alcohol abuse, viral infection and metabolic disorders. Additionally, it is well described that a substantial increase in fibrosis and steatosis frequently leads to fatal cirrhosis and even hepatocellular carcinoma in humans [1]. The high incidence of these hepatopathies places them as one of the most severe diseases. Although the mechanism of some etiologies of liver fibrosis is not fully described, it is clear that reactive oxygen species (ROS) play a key role in the pathogenesis of liver diseases [2]. Increased ROS levels are involved in many pathological conditions and diseases, including cardiovascular disease, diabetes, aging and cancer [3–5]. The repeated administration of carbontetrachloride (CCl<sub>4</sub>) has become one of the most commonly used experimental models for inducing toxin-mediated liver fibrosis [6]. In many aspects, it mimics human chronic disease associated with toxic damage. CCl<sub>4</sub> induces severe liver cell damage through the elevation of ROS, resulting in apoptosis, fibrosis and liver injury that contribute to an acute phase reaction characterized by the necrosis of centrilobular hepatocytes, the activation of Kupffer cells and the induction of an inflammatory response [7]. This sequence is associated with the production of several cytokines that cause liver fibrosis [8]. CCl<sub>4</sub> is metabolized in the liver by the cytochrome P450 superfamily of monooxygenases (CYP family) to the trichloromethyl radical (CCl<sub>3</sub>•). Subsequently, this radical reacts with nucleic acids, proteins and lipids, thereby impairing key cellular processes, resulting in an altered lipid metabolism (fatty degeneration and steatosis). The formation of trichloromethylperoxy radicals (CCl<sub>3</sub>OO•) resulting from the oxygenation of CCl<sub>3</sub>• further initiates lipid peroxidation and the destruction of polyunsaturated fatty acids. Consequently, the membrane permeability in all cellular compartments (mitochondria, endoplasmic reticulum and plasma membrane) is lowered and generalized hepatic damage occurs that is characterized by inflammation, fibrosis and cirrhosis. Biological membranes are particularly prone to the ROS injuries. The peroxidation of fatty acids in cellular membranes induces a decrease in membrane fluidity and disruption of membrane function and integrity, which is involved in severe pathological changes [9]. It is clear that the direct diminution of ROS levels and inhibition of the oxidative chain reaction induced by CCl<sub>4</sub> administration may be critical for the treatment and prevention of CCl<sub>4</sub>-induced liver damage [10]. In fact, it has been previously described that CCl<sub>4</sub> injection increased pro-inflammatory mediators and decreased the antioxidant proteins during liver injury and fibrosis [6,11]. Many endogenous protective mechanisms have been characterized to limit ROS-induced damage [12]. However, additional protective mechanisms of exogenous antioxidants may be important. Thus, many artificial and natural agents possessing antioxidative effects have been suggested to treat and prevent hepatopathies induced by excessive oxidative stress [13,14]. Therefore, supplementation with anti-oxidants is beneficial for human health. Glutathione (γ-L-glutamyl-L-cysteinylglycine, GSH) is an endogenous tripeptide and liver is one of the tissues with the highest content of it. In particular, it is the principal tissue involved in its biosynthesis [15]. Within the cell, GSH is maintained in its thiol-reduced form by an NADPH-dependent enzyme (glutathione disulfide (GSSG) reductase). An additional amount of GSH is present as GSSG and as glutathione conjugates (GS-R). Keeping optimal GSH:GSSG ratios is fundamental for cell survival, since GSH is one of the most important endogenous antioxidant defense systems, removing lipid- and hydrogen-peroxides [16]. A valid approach to replenish the endogenous GSH is using S-acyl prodrugs such as S-acetyl-glutathione (SAG). It is able to cross the cell membrane and increase intracellular SH groups [17]. Differently from GSH, which enters the cells directly, SAG is more stable in blood plasma and, once entered into cell cytoplasm, is converted by cytoplasmatic thioesterases to GSH. In particular, the acetylation of the sulfur atom avoids the GSH decomposition and simplifies its absorption via the intestinal wall [18].

Therefore, in this study, we evaluated the effects of the SAG administration in a mouse model of liver injury, focusing the attention on the CCl<sub>4</sub>-induced fibrosis, oxidative stress, mitophagy and inflammation.

## 2. Results

### 2.1. Effect of SAG on Cytotoxicity and Hepatoprotective Activity in Cells: Preliminary In Vitro Data

Primary hepatic cells only exposed to SAG (0.25–2.00 mM) or the CCl<sub>4</sub> vehicle (DMSO 0.5%) showed no changes in cell viability (Figure 1A). On the other hand, primary hepatic cells exposed to CCl<sub>4</sub> (4 mM) presented a significant reduction in cell viability when compared to the control group. In turn, pre-treatment with all concentrations of SAG followed by exposure to CCl<sub>4</sub> significantly protected against cytotoxicity (Figure 1B).

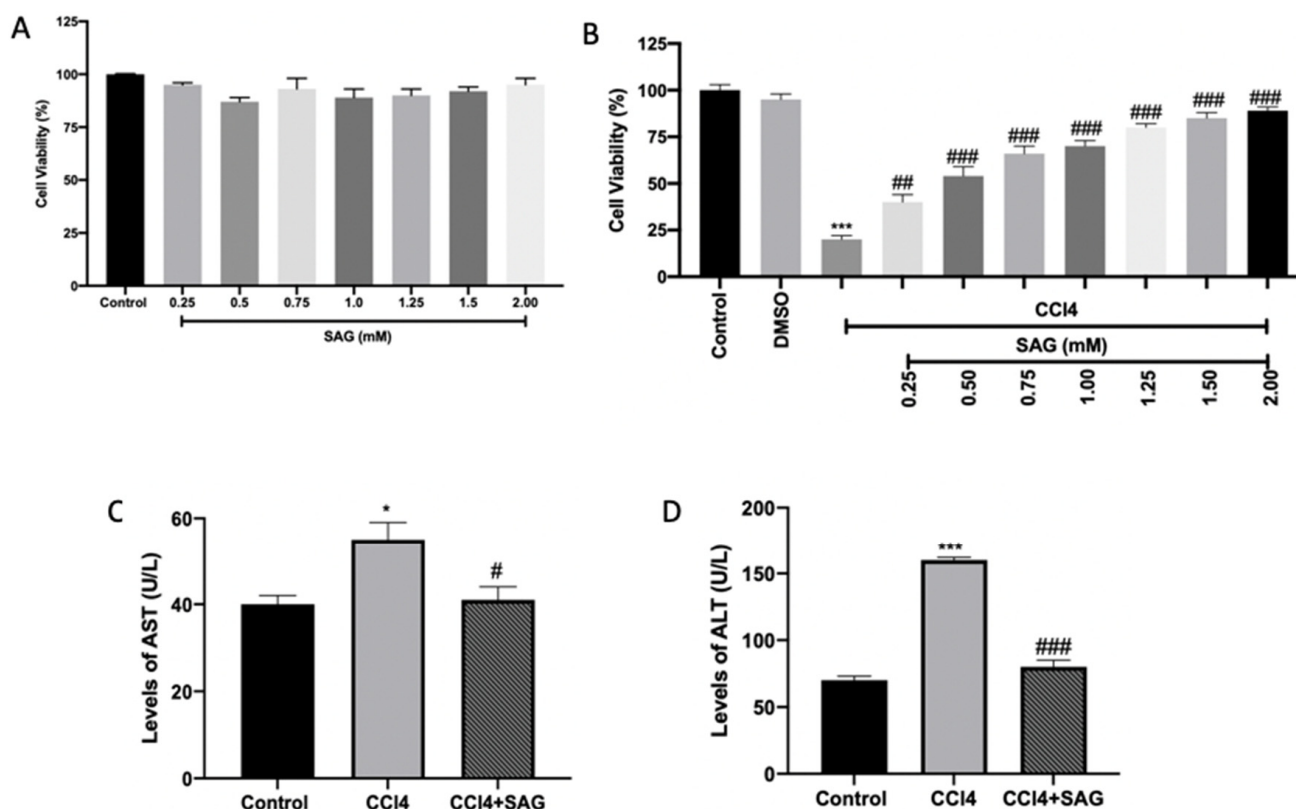


**Figure 1.** Preliminary data on SAG effect on primary hepatic cells: Viability of cells treated with SAG (A); Viability of cells pre-treated for 1 h with SAG followed by exposure to CCl<sub>4</sub> (4 mM) for 6 h (B); Enzymatic activities of AST (C) and ALT (D) in the supernatant. The results were analyzed by one-way ANOVA, followed by a Bonferroni post hoc test for multiple comparisons. A *p*-value of less than 0.05 was considered significant. # *p* < 0.05 vs. control, \* *p* < 0.05 vs. CCl<sub>4</sub>, ## *p* < 0.01 vs. control, ### *p* < 0.001 vs. control, \*\*\* *p* < 0.001 vs. CCl<sub>4</sub>.

In primary hepatic cells exposed to CCl<sub>4</sub>, both AST and ALT levels presented a marked increase, respectively (Figure 1C,D, respectively), in relation to the control group. By contrast, pre-treatment with SAG at 2.00 mM significantly reduced both levels (Figure 1C,D).

### 2.2. Experimental Timeline

CCl<sub>4</sub> is well-known to cause hepatic injury, apoptosis and necrosis [6]. In order to investigate the effects of SAG on hepatic damage, mice were intraperitoneally injected with CCl<sub>4</sub> 1 mL/kg twice a week for 8 consecutive weeks to induce liver fibrosis and were treated orally for 8 weeks with SAG (30 mg/kg) dissolved in saline (Figure 2).

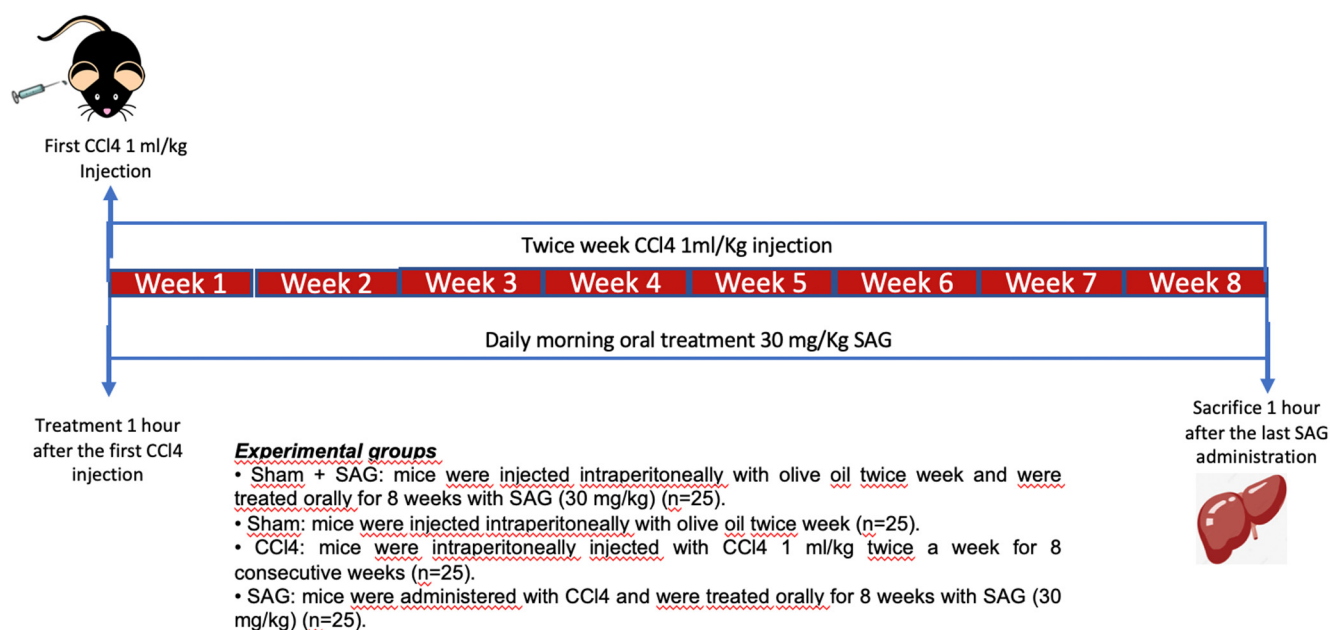


Figure 2. Schematic of study design.

### 2.3. Effects of SAG on Oxidative Stress Induced by CCl4 Chronic Exposure

CCl4 intoxication downregulated SOD (Figure 3A) and GSH (Figure 3B) compared to the sham groups. SAG administration significantly restored SOD activity (Figure 3A) and GSH levels (Figure 3B) in the liver. Additionally, CCl4 administration increased GSSG levels, as compared to the sham groups, whereas it was significantly decreased by SAG administration (Figure 3C). Glutathione peroxidase (GPx) activity was impaired after CCl4 chronic exposure, as compared to the sham groups, whereas SAG administration significantly restored it (Figure 3D). On the same line, SAG supplementation reduced lipid peroxidation (Figure 3E), H<sub>2</sub>O<sub>2</sub> levels (Figure 3F) and ROS levels (Figure 3G) in the samples.

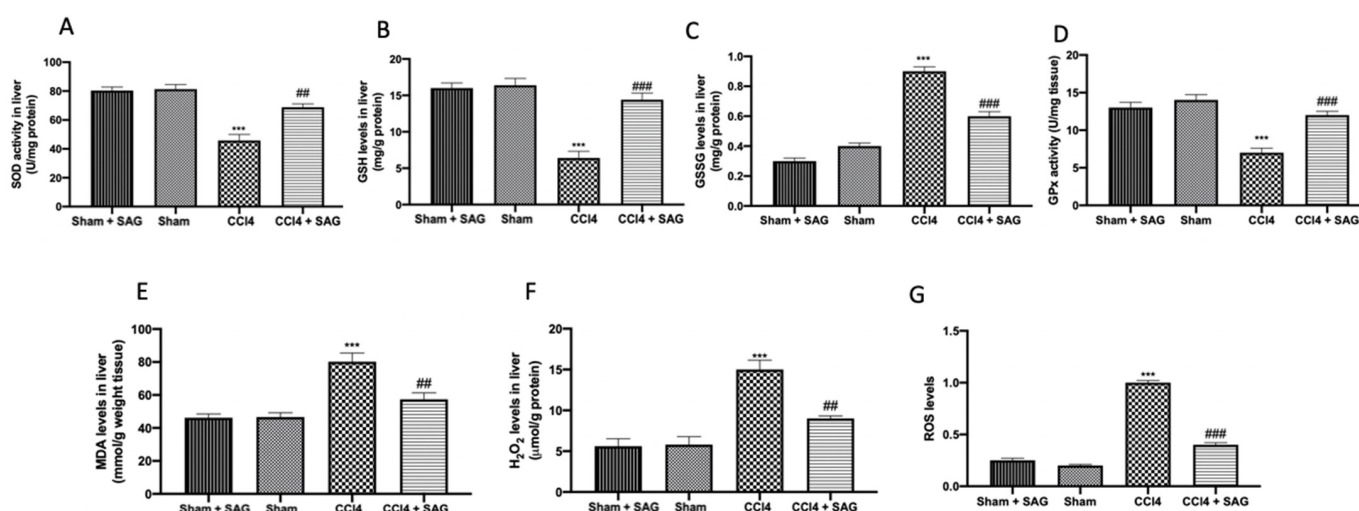
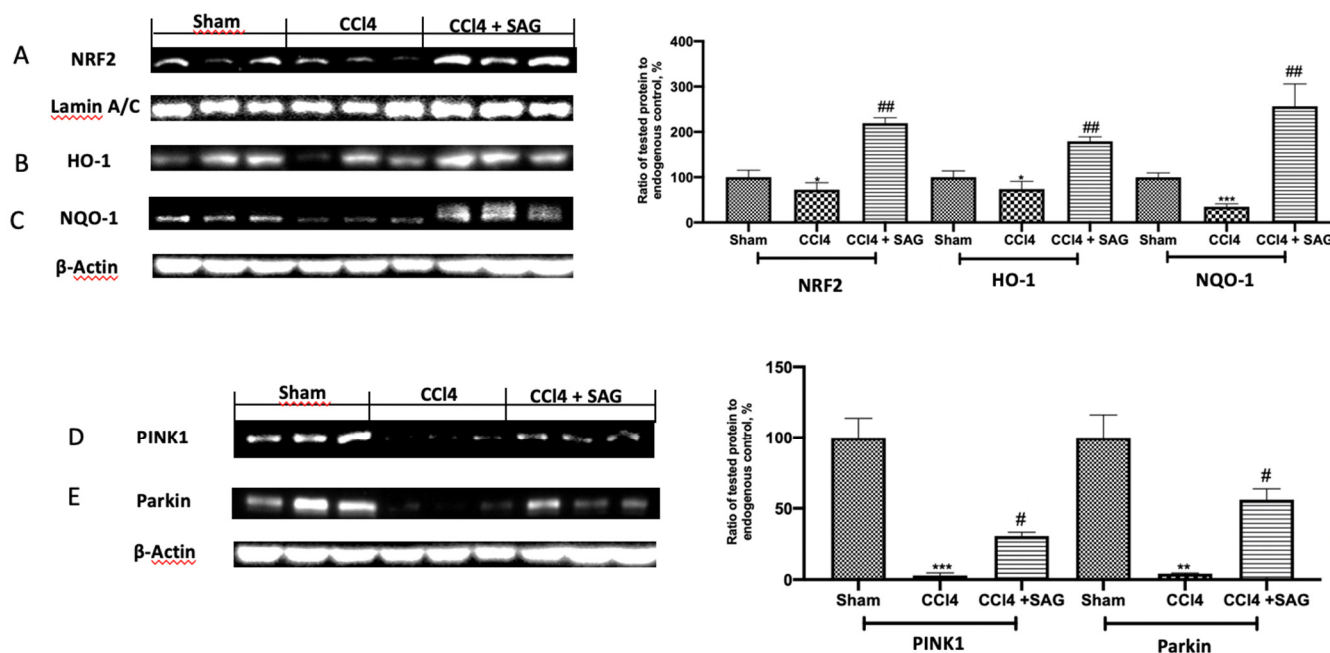


Figure 3. Administration of SAG reduced oxidative stress induced by CCl4 injections: SOD activity (A); GSH levels (B); GSSG levels (C); GPx activity (D); MDA levels (E); H<sub>2</sub>O<sub>2</sub> levels (F); ROS levels (G). For each analysis,  $n = 5$  animals for each group were employed. The results were analyzed by one-way ANOVA, followed by a Bonferroni post hoc test for multiple comparisons. A  $p$ -value of less than 0.05 was considered significant. A  $p$ -value of less than 0.05 was considered significant. \*\*  $p < 0.01$  vs. sham, ###  $p < 0.001$  vs. sham, \*\*\*  $p < 0.001$  vs. CCl4.

#### 2.4. Effects of SAG on Mitophagy Impairments Induced by CCl<sub>4</sub> Chronic Exposure

Western blot analysis displayed that the CCl<sub>4</sub> induced a decrease in anti-oxidants, including Nrf2 (Figure 4A), HO-1 (Figure 4B) and NQO-1 (Figure 4C), which were restored by treatment with SAG. Western blot analysis was also employed to evaluate the effect of SAG on the mitochondrial homeostasis. Chronic CCl<sub>4</sub> exposure impaired mitophagy and mitochondrial biogenesis. PINK1 (Figure 4D) and Parkin (Figure 4E) levels were decreased following CCl<sub>4</sub> intoxication, whereas SAG administration significantly increased their levels.



**Figure 4.** Administration of SAG ameliorated the impaired mitophagy induced by CCl<sub>4</sub> injections: Western blot analysis of: NRF2 (A), HO-1 (B), NQO-1 (C), PINK1 (D) and Parkin (E) levels. For each analysis,  $n = 5$  animals for each group were employed. The results were analyzed by one-way ANOVA, followed by a Bonferroni post hoc test for multiple comparisons. A  $p$ -value of less than 0.05 was considered significant. A  $p$ -value of less than 0.05 was considered significant. #  $p < 0.05$  vs. sham, \*  $p < 0.05$  vs. CCl<sub>4</sub>, ##  $p < 0.01$  vs. sham, \*\*  $p < 0.01$  vs. CCl<sub>4</sub>, \*\*\*  $p < 0.001$  vs. CCl<sub>4</sub>.

#### 2.5. Effects of SAG on Pro-Inflammatory Mediator Secretion Induced by CCl<sub>4</sub> Chronic Exposure

ELISA analysis showed elevated levels of TNF- $\alpha$  (Figure 5A), IL-6 (Figure 5B), IL-1 $\beta$  (Figure 5C) and MCP-1 (Figure 5D) in the liver after CCl<sub>4</sub> intoxication, which were reduced by SAG administration. In addition, the circulating pro-inflammatory cytokines (Figure 5E, 5F and 5G, respectively), as well as the chemokine (Figure 5H), were significantly increased in the CCl<sub>4</sub>-treated mice compared to the sham group. However, mice treated with SAG exhibited a significant downregulation of pro-inflammatory mediators in the serum.

#### 2.6. Effects of SAG on TLR4/NF $\kappa$ B Signaling Activation Induced by CCl<sub>4</sub> Chronic Exposure

In order to confirm SAG anti-inflammatory effects, Western blot analyses were conducted. TLR4 (Figure 6A) and MyD88 (Figure 6B) were significantly increased in CCl<sub>4</sub>-treated mice, as compared to the sham group. SAG administration significantly reduced their expressions. Next, the NF- $\kappa$ B pathway was examined. The sham group showed basal I $\kappa$ B- $\alpha$  cytosolic expression (Figure 6C) and poor nuclear NF- $\kappa$ B p-65 levels (Figure 6D). CCl<sub>4</sub> intoxication importantly degraded cytosolic I $\kappa$ B- $\alpha$  and increased nuclear NF- $\kappa$ B. SAG administration restored I $\kappa$ B- $\alpha$  in cytosol (Figure 6C) and reduced NF- $\kappa$ B nuclear levels (Figure 6D).

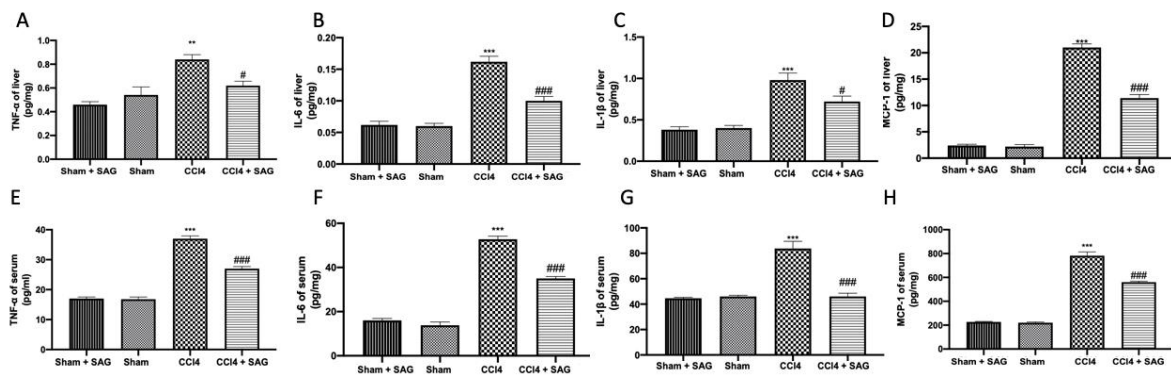


**Figure 5.** Administration of SAG reduced pro-inflammatory mediator secretion induced by CCI4 injections: Liver levels of TNF-α (A), IL-6 (B), IL-1β (C) and MCP-1 (D); Serum levels of TNF-α (E), IL-6 (F), IL-1β (G) and MCP-1 (H). For each analysis,  $n = 5$  animals for each group were employed. The results were analyzed by one-way ANOVA, followed by a Bonferroni post hoc test for multiple comparisons. A  $p$ -value of less than 0.05 was considered significant. A  $p$ -value of less than 0.05 was considered significant. #  $p < 0.05$  vs. sham, \*\*  $p < 0.01$  vs. CCI4, ###  $p < 0.001$  vs. sham, \*\*\*  $p < 0.001$  vs. CCI4.

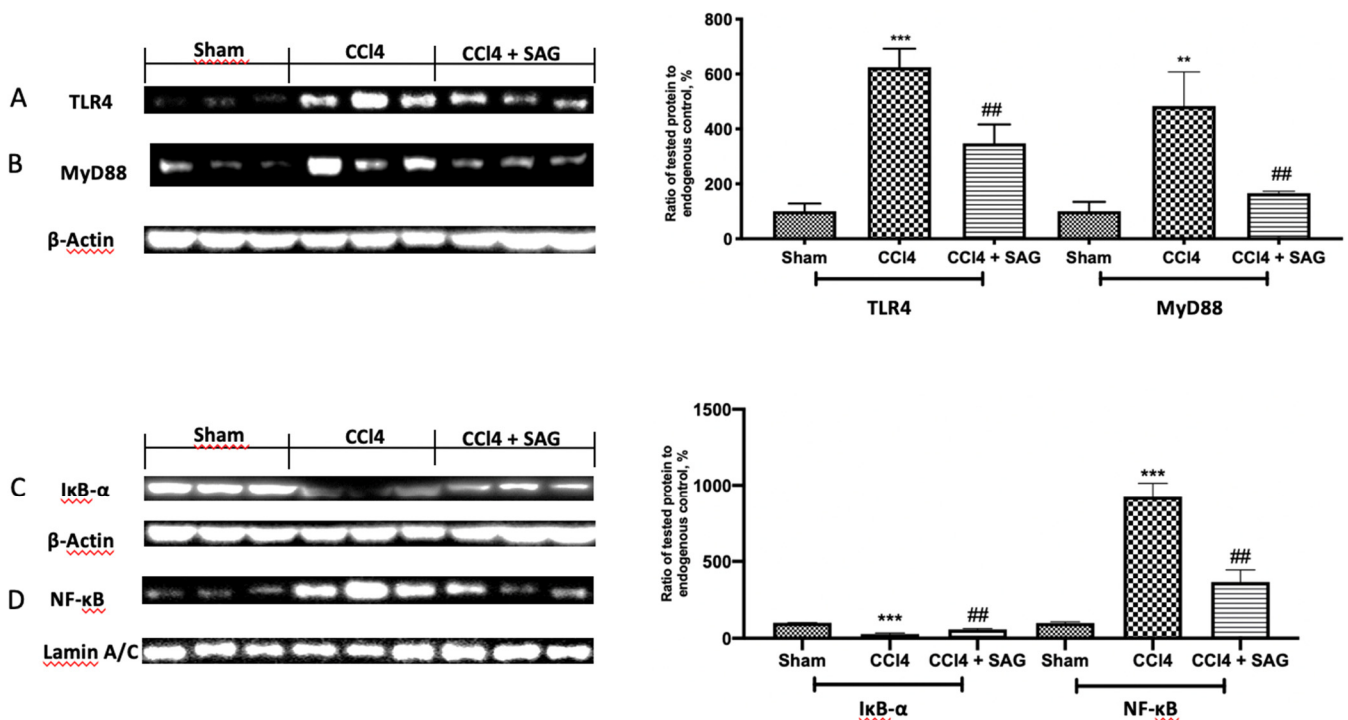


**Figure 6.** Administration of SAG reduced the activation of the TLR4/NF-κB pathway induced by CCI4 injections: Western blot analysis of: TLR4 (A), MyD88 (B), IκB-α (C) and NF-κB (D) levels. For each analysis,  $n = 5$  animals for each group were employed. The results were analyzed by one-way ANOVA, followed by a Bonferroni post hoc test for multiple comparisons. A  $p$ -value of less than 0.05 was considered significant. A  $p$ -value of less than 0.05 was considered significant. ###  $p < 0.01$  vs. sham, \*\*  $p < 0.01$  vs. CCI4, \*\*\*  $p < 0.001$  vs. CCI4.

### 2.7. Effects of SAG on Liver Fibrosis Induced by CCI4 Chronic Exposure

To evaluate fibrosis, CCI4-induced Masson trichrome staining was performed. CCI4-treated animals showed an altered lobule structure through paraplastic connective tissue, and mild to serious fibrosis was detected (Figure 7C,E) compared to the sham group (Figure 7B,E). No differences were assessed between the sham and sham + SAG groups

(Figure 7A,E). An assessment of hydroxyproline was used to test the collagen content in the liver tissue. The hydroxyproline content was also increased in CCl<sub>4</sub>-treated mice (Figure 7F), which was well in line with the upregulated levels of  $\alpha$ -SMA (Figure 7G) and TGF- $\beta$  (Figure 7H), whereas IL10 levels were decreased (Figure 7I) in the liver tissue. SAG administration significantly reduced the collagen deposition (Figure 7D,E), hydroxyproline content (Figure 7F) and  $\alpha$ -SMA (Figure 7G) and TGF- $\beta$  (Figure 7H) levels, whereas it increased IL10 expression (Figure 7I) in the liver tissue. Well in line with the tissue results, TGF- $\beta$  levels (Figure 7J) increased in the serum with CCl<sub>4</sub>, whereas IL10 levels (Figure 7K) decreased. Both levels in the serum were normalized by SAG administration.

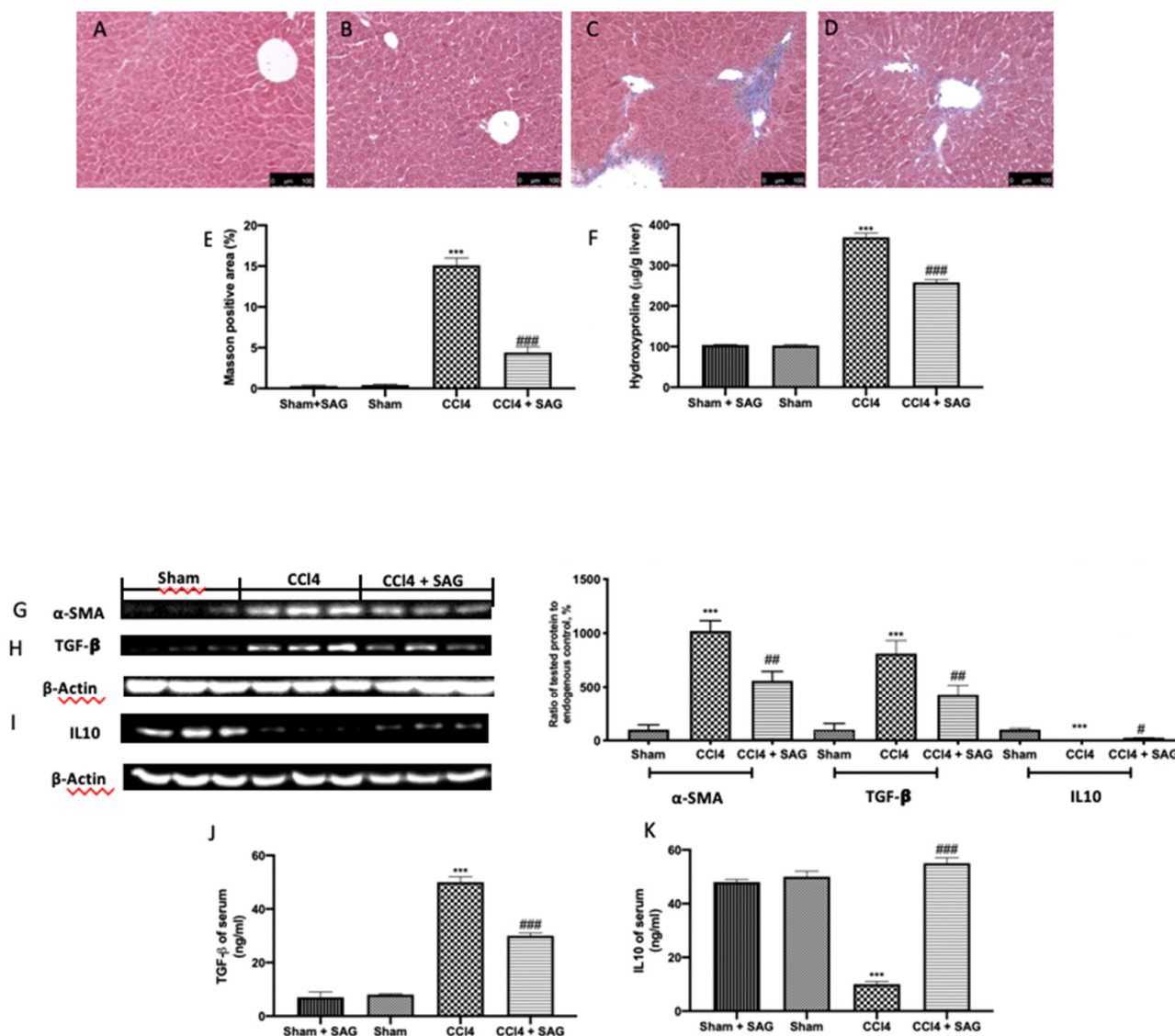


**Figure 7.** Administration of SAG reduced liver fibrosis induced by CCl<sub>4</sub> injections: Masson trichrome staining: Sham + SAG (A), Sham (B), CCl<sub>4</sub> (C), CCl<sub>4</sub> + SAG (D), graphical quantification of Masson-positive area (E); Hydroxyproline content (F); Western blot analysis of:  $\alpha$ -SMA (G), TGF- $\beta$  (H) and IL10 (I) levels in the liver tissue; Serum levels of TGF- $\beta$  (J) and IL10 (K). For each analysis,  $n = 5$  animals for each group were employed. The results were analyzed by one-way ANOVA, followed by a Bonferroni post hoc test for multiple comparisons. A  $p$ -value of less than 0.05 was considered significant. A  $p$ -value of less than 0.05 was considered significant. #  $p < 0.05$  vs. sham, ##  $p < 0.01$  vs. sham, ###  $p < 0.001$  vs. sham, \*\*\*  $p < 0.001$  vs. CCl<sub>4</sub>.

### 2.8. Effects of SAG on Histopathological Alterations and Liver Function Induced by CCl<sub>4</sub> Chronic Exposure

In liver, CCl<sub>4</sub> administration increased the myeloperoxidase (MPO) activity, which is used as an indicator of polymorphonuclear (PMN) cell infiltration (Figure 8F), liver cell damage and necrosis (Figure 8C,E), whereas the sham (Figure 8B,E) and sham + SAG (Figure 8A,E) groups showed normal histological architecture. CCl<sub>4</sub> intoxication also compromised liver function, as shown by ALT (Figure 8G) and AST (Figure 8H) levels. SAG administration significantly ameliorated histological damage (Figure 8D,E), MPO activity (Figure 8F) and liver function (Figure 8G,H).

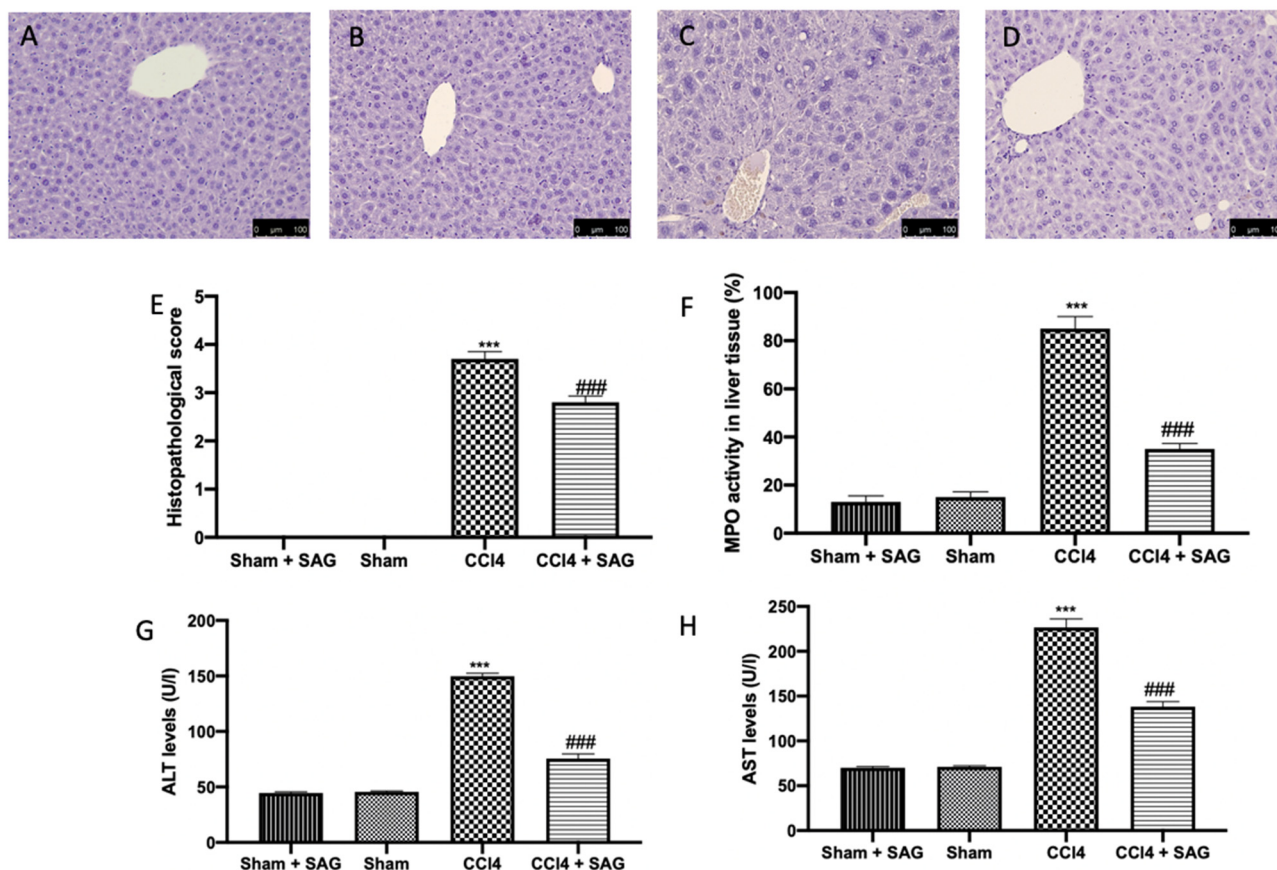


**Figure 8.** Administration of SAG reduced histological changes and liver dysfunction induced by CCl<sub>4</sub> injections: Histological analysis: Sham + SAG (A), Sham (B), CCl<sub>4</sub> (C), CCl<sub>4</sub> + SAG (D), Histological score (E); MPO activity (F); ALT (G) and AST (H) levels. For each analysis,  $n = 5$  animals for each group were employed. The results were analyzed by one-way ANOVA, followed by a Bonferroni post hoc test for multiple comparisons. A  $p$ -value of less than 0.05 was considered significant. A  $p$ -value of less than 0.05 was considered significant. ###  $p < 0.001$  vs. sham, \*\*\*  $p < 0.001$  vs. CCl<sub>4</sub>.

### 3. Discussion

Liver is an important organ involved in several activities, including bile acid secretion, the generation of blood clotting factors and detoxification. Liver injury may be induced by a variety of factors, including drugs, microbes, xenobiotics and several metabolites [19–22]. Previous studies have indicated that increasing GSH plasma levels has beneficial systemic effects [18], well in line with the described GSH depletion in non-alcoholic fatty liver disease patients compared with controls [23]. However, the oral administration of GSH does not significantly enhance GSH in plasma, while GSH derivatives have been described as able to cross the cell membranes and enhance the oral availability. SAG, a GSH precursor, is more stable in plasma, uptaken by cells and later converted to GSH. In this paper, we evaluated the hepatoprotective effects of SAG in a CCl<sub>4</sub>-model of liver injury, in which, the liver

microsomal oxidizing systems related to cytochrome P-450 produce reactive metabolites of CCl<sub>4</sub>, including trichloroperoxy radicals (CCl<sub>3</sub>O<sub>3</sub>·) or trichloromethyl radicals (CCl<sub>3</sub>). These reactive radicals induce lipid peroxidation, causing inflammation and hepatocellular damage and enhancing the production of fibrotic. The pre-treatment of primary hepatic cells with SAG followed by exposure to CCl<sub>4</sub> protected cells against the cytotoxicity, indicating that the extracts counteracted the toxicity of products generated by the metabolism of CCl<sub>4</sub>. This result was corroborated by the analysis of ALT and AST liver enzymes, which overflow to the extracellular medium due to membrane permeability alterations after cellular injury. As expected, exposure to CCl<sub>4</sub> induced a marked release of ALT and AST in primary hepatic cells, while the pre-treatment with SAG promoted the normalization of liver enzyme levels, indicating the protection of the cell membrane. SAG administration, thanks to its ability to maintain a cellular reductive state, enhanced antioxidants, including Nrf2, HO-1 and NQO-1, and restored SOD activity and GSH levels in the liver as well. SAG also reduced GSSG levels, lipid peroxidation and H<sub>2</sub>O<sub>2</sub> liver levels. Accordingly, recent evidence focused the attention on the importance of the mitochondrial dysfunction induced by the sustained ROS in liver fibrosis [24]. Mitophagy is a useful mechanism that aims to remove impaired mitochondria, and is activated by organelle membrane depolarization [25]. Once activated, this mechanism leads to PINK1 stabilization on the mitochondrial outer membrane and to Parkin recruitment from cytosol. The increased oxidative stress characteristic on liver dysfunction causes the impairment of mitophagy and accumulation of dysfunctional and damaged mitochondria. A failure of mitophagy or mitochondrial biogenesis affects hepatocellular function during ischemia/reperfusion [26] and cholestasis [27]. Moreover, interplay between these processes and oxidative metabolism, which may contribute to hepatic cell damage, has been suggested to occur in the steatotic liver [28,29].

Our results showed the protective effect of SAG administration in restoring mitophagy, as shown by the increased PINK1 and Parkin expressions in livers exposed to CCl<sub>4</sub> intoxication. As already shown [30,31], CCl<sub>4</sub> damage is closely associated with inflammation [32]. SAG administration strongly decreased pro-inflammatory cytokines TNF- $\alpha$ , IL-6, MCP-1 and IL-1 $\beta$  in both the serum and liver. This cytokine release is induced by several pathways, including the TLR4/MyD88, a well-known signaling involved in the CCl<sub>4</sub>-induced liver injury. In particular, TLR4 recruits the specific mediator MyD88, which triggers downstream signaling events for the NF $\kappa$ B phosphorylation and a consequent release of pro-inflammatory cytokines [33,34]. ROS interacts with NF- $\kappa$ B signaling pathways in many ways. The transcription of NF- $\kappa$ B-dependent genes influences the levels of ROS in the cell, and, in turn, the levels of NF- $\kappa$ B activity are also regulated by the levels of ROS [35]. NF $\kappa$ B is a transcription factor normally located in the cytoplasm and bound to the IKK complex. Thanks to the activation of the TLR4 pathway, I $\kappa$ B- $\alpha$  is phosphorylated and degraded by proteasome, leading to NF $\kappa$ B release and translocation into the nucleus to increase the expression of targeting genes implicated in the inflammatory response [36,37]. Reducing inflammation and oxidative stress, SAG administration importantly reduced liver fibrosis, as confirmed by the decreased collagen deposition, assessed by Masson trichrome staining, and the reduced hydroxyproline contents and  $\alpha$ -sma and TGF- $\beta$  expressions, while it restored IL10 levels. Consequently, SAG administration attenuated histological liver damage, assessed by hematoxylin and eosin staining; MPO activity, used as an indicator of PMN cell infiltration [38–40]; and improved hepatic function, as shown by ALT and AST levels.

In conclusion, the present study indicated the potential protective effects of SAG against CCl<sub>4</sub>-induced liver damage. The hepatoprotective effects of SAG depend on its ability to reduce the generation of ROS, as well as pro-inflammatory signaling through the de-activation of TLR4/NF- $\kappa$ B signaling (Figure 9). Overall, the present study provides evidence for the protective effects of SAG against CCl<sub>4</sub>-induced liver injury and suggests SAG as a potential hepatoprotective agent used to prevent oxidative liver damage.

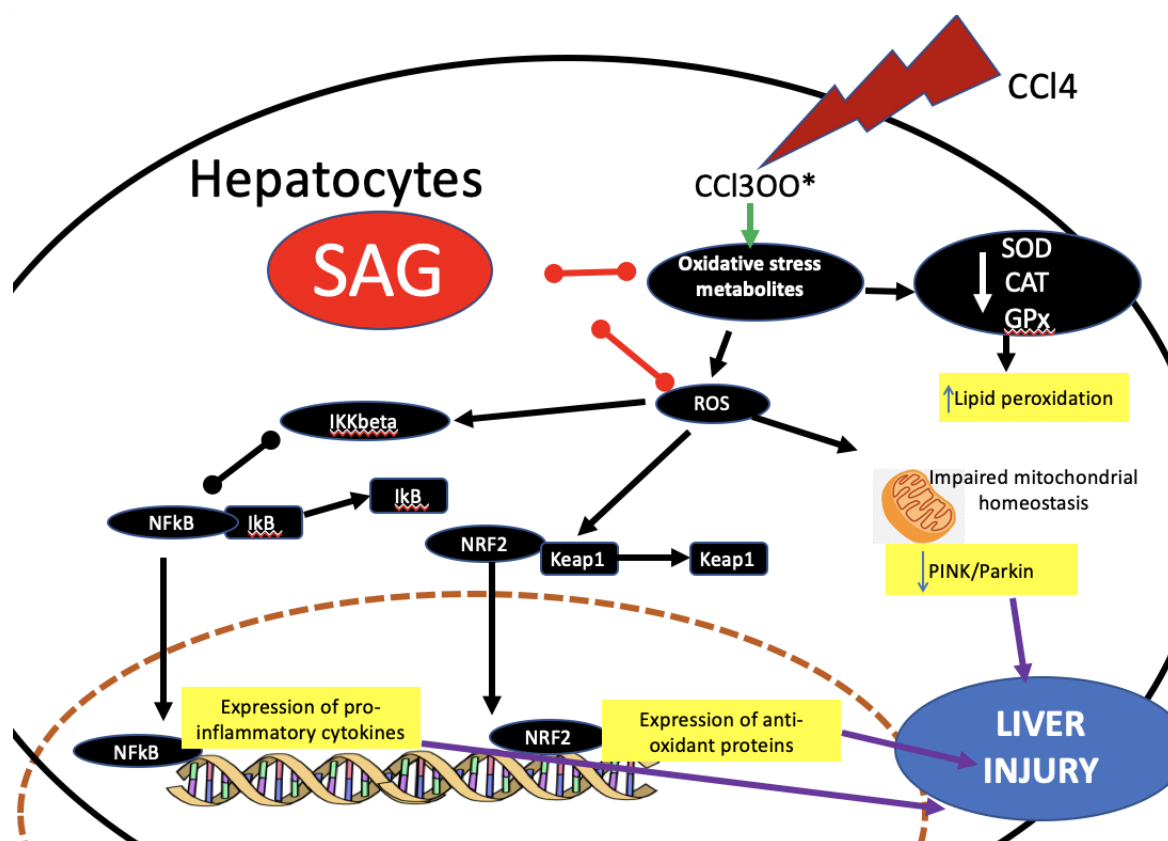


Figure 9. Graphical summary of SAG mechanism.

#### 4. Materials and Methods

##### 4.1. Culture of Hepatocytes

Isolated hepatocytes were prepared from male C57BL/6 mice by the collagenase digestion [41]. Cells were purified by several centrifugations and cultured in DMEM medium supplemented with 10% FBS, HEPES (4.5 mM), penicillin (100 U/mL), L-glutamine (2 mM) and sodium bicarbonate (0.17 M). Cells were maintained under standard culture conditions at 37 °C and 5% CO<sub>2</sub> in a humid environment and trypsinized for experiments whenever the cellular confluence was 70%.

##### 4.2. Cytotoxicity Assay

The assessment of the hepatoprotective effect of SAG was performed using the 3-[4,5-dimethylthiazol-2-yl]-2,5-diphenyl tetrazolium bromide (MTT) reduction assay [42].

Cells (1 × 10<sup>5</sup> cells/well) were seeded in 96-well plates and maintained for 24 h in culture conditions in order to adhere to them. The experimental design involved pre-treatment of primary hepatic cells with SAG (at 0.25, 0.5, 0.75, 1.0, 1.25, 1.5 or 2.00 mM, dissolved in saline as stock solution and diluted in DMEM) for 1 h followed by exposure to CCl<sub>4</sub> (4 mM diluted in 0.5% DMSO) for 6 h. Control group was carried out without CCl<sub>4</sub> exposure. At the exposure time, the medium was exchanged and, after 21 h, 10 µL of MTT (5 mg/mL) was added to each well, and the plates were incubated for 3 h in culture conditions. Supernatants were removed and 100 µL of DMSO was added to each well to solubilize the formazan crystals. The absorbance was measured on a microplate reader at 570 nm.

##### 4.3. Activities of ALT and AST in Cell Supernatants

An evaluation of the activities of the liver-specific enzymes alanine aminotransferase (ALT) and aspartate aminotransferase (AST) is recommended for the assessment of hepa-

tocellular function [43]. For this purpose, primary hepatic cells ( $1 \times 10^6$  cells/well) were seeded in 24-well plates, incubated for 24 h in culture conditions and subsequently pre-treated with SAG (at 2.00 mM) followed by exposure to CCl<sub>4</sub>. Afterwards, supernatants were collected and centrifuged at 5000 rpm for 5 min using a microtube centrifuge. Analyses of the enzymatic activities of AST and ALT were performed according to the manufacturer's instructions (Sigma-Aldrich, Milan, Italy).

#### 4.4. Animals

Sprague Dawley male rats (250 gr, Envigo, Milan, Italy) and C57BL/6 mice (male 20–22 g; age 6–8 weeks) were purchased from Envigo (Milan, Italy) and employed for this study. Messina University Review Board for the carefulness of animals permitted the research (211/2021-PR). All animal experiments agree with the new regulations in Italy (D.Lgs 2014/26), EU regulations (EU Directive 2010/63).

#### 4.5. Carrageenan-Induced Paw Edema (Preliminary Data)

Carrageenan-induced paw edema was performed as previously indicated by a sub-plantar injection of carrageenan (0.1 mL/rat of a 1% suspension in saline) (Sigma-Aldrich, Milan, Italy) into the right hind paw [44]. Increase in paw volume (mL) was measured using a plethysmometer (Ugo Basile, Varese, Italy) immediately prior to the carrageenan injection and every hour for 6 h (Supplemental Figure S1).

#### 4.6. Experimental Groups

Respectively, mice were randomly assigned to different groups, as described below:

- Sham + SAG: mice were injected intraperitoneally with olive oil twice a week and were treated orally for 8 weeks with SAG (30 mg/kg) (Merk, CAS n 3054-47-5, AMBH95E07091) dissolved in saline.
- Sham: mice were injected intraperitoneally with olive oil twice a week.
- CCl<sub>4</sub>: mice were intraperitoneally injected with CCl<sub>4</sub> 1 mL/kg (diluted at 1:10 in olive oil) twice a week for 8 consecutive weeks to induce liver fibrosis [11].
- SAG: mice were administered with CCl<sub>4</sub> to induce liver fibrosis as vehicle group and were treated orally for 8 weeks with SAG (30 mg/kg) dissolved in saline.

At the end of the experiment, blood samples and liver tissues were collected from the mice for further assays. The dose of SAG has been chosen based on experiments previously conducted in our laboratory.

#### 4.7. Analysis of Biochemical Indicators

Serum alanine aminotransferase (ALT) and aspartate aminotransferase (AST) levels were determined according to manufacturer's instructions (Sigma-Aldrich). As for the hepatic hydroxyproline content, snap-frozen liver specimens were collected and the hydroxyproline content was quantified following the manufacturer's instructions (Sigma-Aldrich) [11]. Determination of SOD activity was performed as already described [45]. SOD activity (U/ $\mu$ g protein) was determined using a microplate reader at 560 nm [46]. GSH levels were determined using a microplate reader at 412 nm and expressed as ng/mg wet tissue [45]. GSSG levels were determined using a microplate reader at 450 nm and expressed as ng/mg wet tissue (MyBiosource MBS749109). Glutathione peroxidase activity was estimated by measuring the oxidation of guaiacol in the liver of treated mice according to a standard method [47]. Lipoperoxidation was estimated using the thiobarbituric acid reactive substances (TBARS) test [48]. Briefly, liver tissue was weighed and homogenized in a 1.15% (*w/v*) KCl solution. A 100 mL aliquot of homogenate was then removed and added to a reaction mixture containing 200 mL 8.1% (*w/v*) lauryl sulfate, 1.5 mL 20% (*v/v*) acetic acid (pH 3.5), 1.5 mL 0.8% (*w/v*) thiobarbituric acid and 700 mL distilled water. Samples were then boiled for one hour at 95 °C and centrifuged at 3000 $\times$  *g* for 10 min. The absorbance of the supernatant was measured spectrophotometrically at 532 nm. MDA

levels were expressed as nmol/g wet tissue weight. Whole liver-derived lysates were diluted according to the manufacturer instruction (E-BC-K102-S) and incubated with ammonium molybdate reagent.  $H_2O_2$  content can be calculated by measuring the absorbance value at 405 nm. Relative level of ROS was detected centrifuging liver tissue in the appropriate buffer (20 mmol/L Tris-HCl (pH 7.4), 20 mmol/L  $NaH_2PO_4$ , 5 mmol/L  $MgCl_2$ , 130 mmol/L KCl and 30 mmol/L glucose) and incubating the supernatant with DCFH-DA (2', 7'-dichlorodihydrofluorescein diacetate) for 15 min at 37 °C. Then, the reaction was terminated by adding 1 micromol/L of  $H_2O_2$ . The absorbance value was determined by fluorescence spectrophotometer [49].

#### 4.8. Determination of Myeloperoxidase Activity

MPO activity in liver tissue was used as an indicator of polymorphonuclear (PMN) cell infiltration using a method previously described [50]. Briefly, tissue was weighed and homogenized in a solution containing 0.5% (*w/v*) hexadecyltrimethylammonium bromide dissolved in 10 mmol/L potassium phosphate buffer (pH 7.4) and centrifuged for 30 min at  $20,000 \times g$  at 4 °C. An aliquot of supernatant was then removed and added to a reaction mixture containing 1.6 mmol/L tetramethylbenzidine and 0.1 mmol/L hydrogen peroxide ( $H_2O_2$ ). The rate of change in absorbance was measured spectrophotometrically at 650 nm.

#### 4.9. ELISA

The levels of tumor necrosis factor (TNF)- $\alpha$ , interleukin (IL)-1 $\beta$ , IL-6 and monocyte chemoattractant protein (MCP)-1 in serum and liver tissue samples were determined by ELISA kits (R&D systems) [51]. The levels of TGF- $\beta$  and IL10 in serum were determined by ELISA kits (R&D systems) [52].

#### 4.10. Histopathological Examination

For histopathological investigations, liver tissues were fixed in formaldehyde solution (10% in PBS); histological sections were stained with hematoxylin and eosin (H&E) and evaluated using a Leica DM6 microscope (Leica Microsystems SpA, Milan, Italy) equipped with a motorized stage and associated with Leica LAS X Navigator software (Leica Microsystems SpA, Milan, Italy) [53]. Histopathologic scores were graded following the Ishak scoring system as follows: 0, no fibrosis; 1, fibrosis expansion of some portal areas  $\pm$  short fibrous septa; 2, fibrosis expansion of portal areas  $\pm$  short fibrous septa; 3, fibrosis expansion of most portal areas with occasional portal to portal bridging; 4, fibrosis expansion of portal areas with marked portal to portal bridging, as well as portal to central; 5, marked bridging with occasional nodules (incomplete cirrhosis); 6, cirrhosis, probable or definite [54–56]. Collagen deposition was evaluated by Masson trichrome staining performed according to the manufacturer's protocol (Bio-Optica, Milan, Italy) [57].

#### 4.11. Western Blot Analysis

Western blot analyses were made as previously described [58]. Filters were blocked with  $1 \times$  PBS, 5% (*w/v*) no-fat dried milk (PM) for 40 min at room temperature and then probed with one of the next primary antibodies: anti-TGF- $\beta$  (Santa Cruz Biotechnology, sc-130348), anti-IL-10 (Santa Cruz Biotechnology, sc-8438) or anti-I $\kappa$ B- $\alpha$  (Santa Cruz Biotechnology, sc-1643), or anti-NF- $\kappa$ B p-65 (Santa Cruz Biotechnology, sc-8008), or anti-TLR4 (Santa Cruz Biotechnology, sc-293072), anti-MyD88 (Santa Cruz Biotechnology, sc-74532), or anti- $\alpha$ -SMA (Santa Cruz Biotechnology, sc-53015), or anti-Nrf-2 (Santa Cruz Biotechnology, sc-365949), or anti-HO-1 (Santa Cruz Biotechnology, sc-136960), or NQO-1 (Abcam), or anti-PINK1 (Santa Cruz Biotechnology, sc-517353), or anti-Parkin (Santa Cruz Biotechnology, sc-32282) in  $1 \times$  PBS, 0.1% Tween-20, 5% *w/v* no-fat dried milk (PMT) at 4 °C overnight. Membranes were incubated with peroxidase-conjugated bovine anti-mouse IgG secondary antibody or peroxidase-conjugated goat anti-rabbit IgG (1:2000, Jackson ImmunoResearch, West Grove, PA, USA) [59]. Blots were also incubated with primary antibody against  $\beta$ -actin protein (1:10,000; Sigma-Aldrich Corp.) or lamin (1:10,000; Sigma-Aldrich Corp.),

used as internal standards [60]. The relative expressions of the protein bands were detected and quantified by densitometry, as previously explained [61]. In the experiments including Western blot, a representative blot is displayed and densitometric analysis is related in each figure.

#### 4.12. Statistical Evaluation

All values in the images and text are expressed as mean  $\pm$  standard error of the mean (SEM) of N observations. For in vivo studies, N represents the number of animals. In experiments involving histology and immunohistochemistry, the illustrations represent the outcomes of at least three independent experiments. The results were analyzed by one-way ANOVA, followed by a Bonferroni post hoc test for multiple comparisons. A *p*-value of less than 0.05 was considered significant. A *p*-value of less than 0.05 was considered significant. # *p* < 0.05 vs. sham, \* *p* < 0.05 vs. vehicle, ## *p* < 0.01 vs. sham, \*\* *p* < 0.01 vs. vehicle, ### *p* < 0.001 vs. sham, \*\*\* *p* < 0.001 vs. vehicle.

**Supplementary Materials:** The following supporting information can be downloaded at: <https://www.mdpi.com/article/10.3390/ijms23084429/s1>.

**Author Contributions:** Conceptualization, R.F. and S.C.; methodology, A.T.S.; software, M.C.; validation, R.S.; formal analysis, R.D.; investigation, D.I.; resources, M.L.O.; data curation, S.M. and L.I.; writing—original draft preparation, R.F.; writing—review and editing, R.D.P.; supervision, V.C.; project administration, R.D.P.; funding acquisition, S.C. All authors have read and agreed to the published version of the manuscript.

**Funding:** This research received no external funding.

**Institutional Review Board Statement:** The University of Messina Review Board for animal care. (OPBA) approved the study. All animal experiments agreed with the new Italian regulations (D.Lgs 2014/26), EU regulations (EU Directive 2010/63), and the ARRIVE guidelines.

**Informed Consent Statement:** Not applicable.

**Data Availability Statement:** The data used to support the findings of this study are available from the corresponding author upon request.

**Conflicts of Interest:** The authors declare no conflict of interest.

## References

1. Bataller, R.; Brenner, D.A. Liver fibrosis. *J. Clin. Investig.* **2005**, *115*, 209–218. [[CrossRef](#)] [[PubMed](#)]
2. Poli, G.; Parola, M. Oxidative damage and fibrogenesis. *Free Radic. Biol. Med.* **1997**, *22*, 287–305. [[CrossRef](#)]
3. Harrison, D.G.; Cai, H.; Landmesser, U.; Griendling, K.K. Interactions of angiotensin II with NAD (P) H oxidase, oxidant stress and cardiovascular disease. *J. Renin-Angiotensin-Aldosterone Syst.* **2003**, *4*, 51–61. [[CrossRef](#)] [[PubMed](#)]
4. Inoguchi, T.; Sonta, T.; Tsubouchi, H.; Etoh, T.; Kakimoto, M.; Sonoda, N.; Sato, N.; Sekiguchi, N.; Kobayashi, K.; Sumimoto, H. Protein kinase C-dependent increase in reactive oxygen species (ROS) production in vascular tissues of diabetes: Role of vascular NAD (P) H oxidase. *J. Am. Soc. Nephrol.* **2003**, *14*, S227–S232. [[CrossRef](#)] [[PubMed](#)]
5. Singh, K.K. Mitochondrial dysfunction is a common phenotype in aging and cancer. *Ann. N. Y. Acad. Sci.* **2004**, *1019*, 260–264. [[CrossRef](#)] [[PubMed](#)]
6. Scholten, D.; Trebicka, J.; Liedtke, C.; Weiskirchen, R. The carbon tetrachloride model in mice. *Lab. Anim.* **2015**, *49*, 4–11. [[CrossRef](#)] [[PubMed](#)]
7. Heindryckx, F.; Colle, I.; Van Vlierberghe, H. Experimental mouse models for hepatocellular carcinoma research. *Int. J. Exp. Pathol.* **2009**, *90*, 367–386. [[CrossRef](#)]
8. Iwaisako, K.; Jiang, C.; Zhang, M.; Cong, M.; Moore-Morris, T.J.; Park, T.J.; Liu, X.; Xu, J.; Wang, P.; Paik, Y.H.; et al. Origin of myofibroblasts in the fibrotic liver in mice. *Proc. Natl. Acad. Sci. USA* **2014**, *111*, E3297–E3305. [[CrossRef](#)]
9. Halliwell, B. Oxidants and human disease: Some new concepts. *FASEB J.* **1987**, *1*, 358–364. [[CrossRef](#)]
10. Bosek, P.; Nakano, M. Hepatoprotective effect of rooibos tea (*Aspalathus linearis*) on CCl<sub>4</sub>-induced liver damage in rats. *Physiol. Res.* **2003**, *52*, 461–466.
11. Liu, Y.; Wen, P.H.; Zhang, X.X.; Dai, Y.; He, Q. Breviscapine ameliorates CCl<sub>4</sub>-induced liver injury in mice through inhibiting inflammatory apoptotic response and ROS generation. *Int. J. Mol. Med.* **2018**, *42*, 755–768. [[PubMed](#)]
12. Sies, H. Strategies of antioxidant defense. *Eur. J. Biochem.* **1993**, *215*, 213–219. [[CrossRef](#)] [[PubMed](#)]

13. Lieber, C.S. Role of oxidative stress and antioxidant therapy in alcoholic and nonalcoholic liver diseases. *Adv. Pharmacol.* **1997**, *38*, 601–628. [[PubMed](#)]
14. Cervinkova, Z.; Drahotova, Z. Enteral administration of lipid emulsions protects liver cytochrome c oxidase from hepatotoxic action of thioacetamide. *Physiol. Res.* **1998**, *47*, 151–154.
15. Lu, S.C. Regulation of hepatic glutathione synthesis: Current concepts and controversies. *FASEB J.* **1999**, *13*, 1169–1183. [[CrossRef](#)]
16. Meister, A.; Anderson, M.E. Glutathione. *Annu. Rev. Biochem.* **1983**, *52*, 711–760. [[CrossRef](#)]
17. Vogel, J.-U.; Cinatl, J.; Dauletbaev, N.; Buxbaum, S.; Treusch, G.; Cinatl, J.; Gerein, V.; Doerr, H.W. Effects of S-acetylglutathione in cell and animal model of herpes simplex virus type 1 infection. *Med. Microbiol. Immunol.* **2005**, *194*, 55–59. [[CrossRef](#)]
18. Fanelli, S.; Francioso, A.; Cavallaro, R.A.; d’Erme, M.; Putignano, P.; Miraglia, N.; Mosca, L. Clinical Nutrition & Dietetics. *Clin. Nutr. Diet.* **2018**, *4*, 134.
19. Rowland, A.; Miners, J.O.; Mackenzie, P.I. The UDP-glucuronosyltransferases: Their role in drug metabolism and detoxification. *Int. J. Biochem. Cell Biol.* **2013**, *45*, 1121–1132. [[CrossRef](#)]
20. Mao, S.; Gao, D.; Liu, W.; Wei, H.; Lin, J.M. Imitation of drug metabolism in human liver and cytotoxicity assay using a microfluidic device coupled to mass spectrometric detection. *Lab Chip* **2012**, *12*, 219–226. [[CrossRef](#)]
21. Dawson, S.; Stahl, S.; Paul, N.; Barber, J.; Kenna, J.G. In Vitro inhibition of the bile salt export pump correlates with risk of cholestatic drug-induced liver injury in humans. *Drug Metab. Dispos.* **2012**, *40*, 130–138. [[CrossRef](#)] [[PubMed](#)]
22. Luyendyk, J.P.; Kassel, K.M.; Allen, K.; Guo, G.L.; Li, G.; Cantor, G.H.; Copple, B.L. Fibrinogen deficiency increases liver injury and early growth response-1 (Egr-1) expression in a model of chronic xenobiotic-induced cholestasis. *Am. J. Pathol.* **2012**, *178*, 1117–1125. [[CrossRef](#)] [[PubMed](#)]
23. Videla, L.A.; Rodrigo, R.; Orellana, M.; Fernandez, V.; Tapia, G.; Quinones, L.; Varela, N.; Contreras, J.; Lazarte, R.; Csendes, A.; et al. Oxidative stress-related parameters in the liver of non-alcoholic fatty liver disease patients. *Clin. Sci.* **2004**, *106*, 261–268. [[CrossRef](#)] [[PubMed](#)]
24. Casalena, G.; Daehn, I.; Bottinger, E. Transforming growth factor-beta, bioenergetics, and mitochondria in renal disease. *Semin. Nephrol.* **2012**, *32*, 295–303. [[CrossRef](#)] [[PubMed](#)]
25. Kubli, D.A.; Gustafsson, A.B. Mitochondria and mitophagy: The yin and yang of cell death control. *Circ. Res.* **2012**, *111*, 1208–1221. [[CrossRef](#)]
26. Czaja, M.J.; Ding, W.X.; Donohue, T.M., Jr.; Friedman, S.L.; Kim, J.S.; Komatsu, M.; Lemasters, J.J.; Lemoine, A.; Lin, J.D.; Ou, J.H.; et al. Functions of autophagy in normal and diseased liver. *Autophagy* **2013**, *9*, 1131–1158. [[CrossRef](#)]
27. Serviddio, G.; Bellanti, F.; Stanca, E.; Lunetti, P.; Blonda, M.; Tamborra, R.; Siculella, L.; Vendemiale, G.; Capobianco, L.; Giudetti, A.M. Silybin exerts antioxidant effects and induces mitochondrial biogenesis in liver of rat with secondary biliary cirrhosis. *Free Radic. Biol. Med.* **2014**, *73*, 117–126. [[CrossRef](#)]
28. Kim, C.S.; Kwon, Y.; Choe, S.Y.; Hong, S.M.; Yoo, H.; Goto, T.; Kawada, T.; Choi, H.S.; Joe, Y.; Chung, H.T.; et al. Quercetin reduces obesity-induced hepatosteatosis by enhancing mitochondrial oxidative metabolism via heme oxygenase-1. *Nutr. Metab.* **2015**, *12*, 33. [[CrossRef](#)]
29. Cavalheri, H.; Both, C.; Martins, M. The Interplay between Environmental Filtering and Spatial Processes in Structuring Communities: The Case of Neotropical Snake Communities. *PLoS ONE* **2015**, *10*, e0127959. [[CrossRef](#)]
30. Poling, J.; Gajawada, P.; Richter, M.; Lorchner, H.; Polyakova, V.; Kostin, S.; Shin, J.; Boettger, T.; Walther, T.; Rees, W.; et al. Therapeutic targeting of the oncostatin M receptor-beta prevents inflammatory heart failure. *Basic Res. Cardiol.* **2014**, *109*, 396. [[CrossRef](#)]
31. Szepechcinski, A.; Chorostowska-Wynimko, J.; Struniawski, R.; Kupis, W.; Rudzinski, P.; Langfort, R.; Puscinska, E.; Bielen, P.; Sliwinski, P.; Orłowski, T. Cell-free DNA levels in plasma of patients with non-small-cell lung cancer and inflammatory lung disease. *Br. J. Cancer* **2015**, *113*, 476–483. [[CrossRef](#)] [[PubMed](#)]
32. Shi, H.; Dong, L.; Jiang, J.; Zhao, J.; Zhao, G.; Dang, X.; Lu, X.; Jia, M. Chlorogenic acid reduces liver inflammation and fibrosis through inhibition of toll-like receptor 4 signaling pathway. *Toxicology* **2013**, *303*, 107–114. [[CrossRef](#)] [[PubMed](#)]
33. Zhu, H.T.; Bian, C.; Yuan, J.C.; Chu, W.H.; Xiang, X.; Chen, F.; Wang, C.S.; Feng, H.; Lin, J.K. Curcumin attenuates acute inflammatory injury by inhibiting the TLR4/MyD88/NF-kappaB signaling pathway in experimental traumatic brain injury. *J. Neuroinflammation* **2014**, *11*, 59. [[CrossRef](#)]
34. Ma, Y.; He, M.; Qiang, L. Exercise Therapy Downregulates the Overexpression of TLR4, TLR2, MyD88 and NF-kappaB after Cerebral Ischemia in Rats. *Int. J. Mol. Sci.* **2013**, *4*, 3718–3733. [[CrossRef](#)] [[PubMed](#)]
35. Morgan, M.J.; Liu, Z.G. Crosstalk of reactive oxygen species and NF-kappaB signaling. *Cell Res.* **2011**, *21*, 103–115. [[CrossRef](#)]
36. Wei, H.Y.; Ma, X. Tamoxifen reduces infiltration of inflammatory cells, apoptosis and inhibits IKK/NF-kB pathway after spinal cord injury in rats. *Neurol. Sci.* **2014**, *35*, 1763–1768. [[CrossRef](#)]
37. Baldwin, A.S. Regulation of cell death and autophagy by IKK and NF-kappaB: Critical mechanisms in immune function and cancer. *Immunol. Rev.* **2012**, *246*, 327–345. [[CrossRef](#)]
38. Di Paola, R.; Cordaro, M.; Crupi, R.; Siracusa, R.; Campolo, M.; Bruschetta, G.; Fusco, R.; Pugliatti, P.; Esposito, E.; Cuzzocrea, S. Protective Effects of Ultramicronized Palmitoylethanolamide (PEA-um) in Myocardial Ischaemia and Reperfusion Injury in vivo. *Shock* **2016**, *46*, 202–213. [[CrossRef](#)]

39. Di Paola, R.; Impellizzeri, D.; Fusco, R.; Cordaro, M.; Siracusa, R.; Crupi, R.; Esposito, E.; Cuzzocrea, S. Ultramicronized palmitoylethanolamide (PEA-um((R))) in the treatment of idiopathic pulmonary fibrosis. *Pharmacol. Res.* **2016**, *111*, 405–412. [[CrossRef](#)]
40. Fusco, R.; Cirmi, S.; Gugliandolo, E.; Di Paola, R.; Cuzzocrea, S.; Navarra, M. A flavonoid-rich extract of orange juice reduced oxidative stress in an experimental model of inflammatory bowel disease. *J. Funct. Foods* **2017**, *30*, 168–178. [[CrossRef](#)]
41. Lee, M.K.; Yeo, H.; Kim, J.; Kim, Y.C. Protection of rat hepatocytes exposed to CCl<sub>4</sub> in-vitro by cynandione A, a biacetophenone from *Cynanchum wilfordii*. *J. Pharm. Pharmacol.* **2000**, *52*, 341–345. [[CrossRef](#)] [[PubMed](#)]
42. de Oliveira Fernandes, T.; de Avila, R.I.; de Moura, S.S.; de Almeida Ribeiro, G.; Naves, M.M.V.; Valadares, M.C. *Campomanesia adamantium* (Myrtaceae) fruits protect HEPG2 cells against carbon tetrachloride-induced toxicity. *Toxicol. Rep.* **2015**, *2*, 184–193. [[CrossRef](#)] [[PubMed](#)]
43. Boone, L.; Meyer, D.; Cusick, P.; Ennulat, D.; Bolliger, A.P.; Everds, N.; Meador, V.; Elliott, G.; Honor, D.; Bounous, D. Selection and interpretation of clinical pathology indicators of hepatic injury in preclinical studies. *Vet. Clin. Pathol.* **2005**, *34*, 182–188. [[CrossRef](#)] [[PubMed](#)]
44. Cordaro, M.; Siracusa, R.; Fusco, R.; D'Amico, R.; Peritore, A.F.; Gugliandolo, E.; Genovese, T.; Scuto, M.; Crupi, R.; Mandalari, G.; et al. Cashew (*Anacardium occidentale* L.) Nuts Counteract Oxidative Stress and Inflammation in an Acute Experimental Model of Carrageenan-Induced Paw Edema. *Antioxidants* **2020**, *9*, 660. [[CrossRef](#)] [[PubMed](#)]
45. Siracusa, R.; D'Amico, R.; Cordaro, M.; Peritore, A.F.; Genovese, T.; Gugliandolo, E.; Crupi, R.; Impellizzeri, D.; Cuzzocrea, S.; Fusco, R.; et al. The Methyl Ester of 2-Cyano-3,12-Dioxooleana-1,9-Dien-28-Oic Acid Reduces Endometrial Lesions Development by Modulating the NFκB and Nrf2 Pathways. *Int. J. Mol. Sci.* **2021**, *22*, 3991. [[CrossRef](#)]
46. Fusco, R.; Cordaro, M.; Siracusa, R.; D'Amico, R.; Genovese, T.; Gugliandolo, E.; Peritore, A.F.; Crupi, R.; Impellizzeri, D.; Cuzzocrea, S.; et al. Biochemical Evaluation of the Antioxidant Effects of Hydroxytyrosol on Pancreatitis-Associated Gut Injury. *Antioxidants* **2020**, *9*, 781. [[CrossRef](#)]
47. Dutta, S.; Chakraborty, A.K.; Dey, P.; Kar, P.; Guha, P.; Sen, S.; Kumar, A.; Sen, A.; Chaudhuri, T.K. Amelioration of CCl<sub>4</sub> induced liver injury in swiss albino mice by antioxidant rich leaf extract of *Croton bonplandianus* Baill. *PLoS ONE* **2018**, *13*, e0196411. [[CrossRef](#)]
48. Siracusa, R.; Fusco, R.; Peritore, A.F.; Cordaro, M.; D'Amico, R.; Genovese, T.; Gugliandolo, E.; Crupi, R.; Smeriglio, A.; Mandalari, G.; et al. The Antioxidant and Anti-Inflammatory Properties of *Anacardium occidentale* L. Cashew Nuts in a Mouse Model of Colitis. *Nutrients* **2020**, *12*, 834. [[CrossRef](#)]
49. Liu, B.; Zhang, J.; Sun, P.; Yi, R.; Han, X.; Zhao, X. Raw Bowl Tea (TuoCha) Polyphenol Prevention of Nonalcoholic Fatty Liver Disease by Regulating Intestinal Function in Mice. *Biomolecules* **2019**, *9*, 435. [[CrossRef](#)]
50. Peritore, A.F.; D'Amico, R.; Cordaro, M.; Siracusa, R.; Fusco, R.; Gugliandolo, E.; Genovese, T.; Crupi, R.; Di Paola, R.; Cuzzocrea, S.; et al. PEA/Polydatin: Anti-Inflammatory and Antioxidant Approach to Counteract DNBS-Induced Colitis. *Antioxidants* **2021**, *10*, 463. [[CrossRef](#)]
51. Cordaro, M.; Siracusa, R.; Impellizzeri, D.; D'Amico, R.; Peritore, A.F.; Crupi, R.; Gugliandolo, E.; Fusco, R.; Di Paola, R.; Schievano, C.; et al. Safety and efficacy of a new micronized formulation of the ALIamide palmitoylglucosamine in preclinical models of inflammation and osteoarthritis pain. *Arthritis Res. Ther.* **2019**, *21*, 254. [[CrossRef](#)] [[PubMed](#)]
52. Saber, S.; Mahmoud, A.A.A.; Helal, N.S.; El-Ahwany, E.; Abdelghany, R.H. Renin-angiotensin system inhibition ameliorates CCl<sub>4</sub>-induced liver fibrosis in mice through the inactivation of nuclear transcription factor kappa B. *Can. J. Physiol. Pharmacol.* **2018**, *96*, 569–576. [[CrossRef](#)] [[PubMed](#)]
53. Peritore, A.F.; Siracusa, R.; Fusco, R.; Gugliandolo, E.; D'Amico, R.; Cordaro, M.; Crupi, R.; Genovese, T.; Impellizzeri, D.; Cuzzocrea, S.; et al. Ultramicronized Palmitoylethanolamide and Paracetamol, a New Association to Relieve Hyperalgesia and Pain in a Sciatic Nerve Injury Model in Rat. *Int. J. Mol. Sci.* **2020**, *21*, 3509. [[CrossRef](#)] [[PubMed](#)]
54. Uesugi, T.; Froh, M.; Arteel, G.E.; Bradford, B.U.; Thurman, R.G. Toll-like receptor 4 is involved in the mechanism of early alcohol-induced liver injury in mice. *Hepatology* **2011**, *34*, 101–108. [[CrossRef](#)]
55. Nallagangula, K.S.; Nagaraj, S.K.; Venkataswamy, L.; Chandrappa, M. Liver fibrosis: A compilation on the biomarkers status and their significance during disease progression. *Future Sci. OA* **2018**, *4*, FSO250. [[CrossRef](#)]
56. Su, T.H.; Shiau, C.W.; Jao, P.; Yang, N.J.; Tai, W.T.; Liu, C.J.; Tseng, T.C.; Yang, H.C.; Liu, C.H.; Huang, K.W.; et al. Src-homology protein tyrosine phosphatase-1 agonist, SC-43, reduces liver fibrosis. *Sci. Rep.* **2017**, *7*, 1728. [[CrossRef](#)]
57. Fusco, R.; Siracusa, R.; Peritore, A.F.; Gugliandolo, E.; Genovese, T.; D'Amico, R.; Cordaro, M.; Crupi, R.; Mandalari, G.; Impellizzeri, D.; et al. The Role of Cashew (*Anacardium occidentale* L.) Nuts on an Experimental Model of Painful Degenerative Joint Disease. *Antioxidants* **2020**, *9*, 511. [[CrossRef](#)]
58. Fusco, R.; Gugliandolo, E.; Siracusa, R.; Scuto, M.; Cordaro, M.; D'Amico, R.; Evangelista, M.; Peli, A.; Peritore, A.F.; Impellizzeri, D.; et al. Formyl Peptide Receptor 1 Signaling in Acute Inflammation and Neural Differentiation Induced by Traumatic Brain Injury. *Biology* **2020**, *9*, 238. [[CrossRef](#)]
59. D'Amico, R.; Fusco, R.; Cordaro, M.; Siracusa, R.; Peritore, A.F.; Gugliandolo, E.; Crupi, R.; Scuto, M.; Cuzzocrea, S.; Di Paola, R.; et al. Modulation of NLRP3 Inflammasome through Formyl Peptide Receptor 1 (Fpr-1) Pathway as a New Therapeutic Target in Bronchiolitis Obliterans Syndrome. *Int. J. Mol. Sci.* **2020**, *21*, 2144. [[CrossRef](#)]

60. Esposito, E.; Campolo, M.; Casili, G.; Lanza, M.; Franco, D.; Filippone, A.; Peritore, A.F.; Cuzzocrea, S. Protective Effects of Xyloglucan in Association with the Polysaccharide Gelose in an Experimental Model of Gastroenteritis and Urinary Tract Infection. *Int. J. Mol. Sci.* **2018**, *19*, 1844. [[CrossRef](#)]
61. Fusco, R.; Cordaro, M.; Genovese, T.; Impellizzeri, D.; Siracusa, R.; Gugliandolo, E.; Peritore, A.F.; D'Amico, R.; Crupi, R.; Cuzzocrea, S.; et al. Adelmidrol: A New Promising Antioxidant and Anti-Inflammatory Therapeutic Tool in Pulmonary Fibrosis. *Antioxidants* **2020**, *9*, 601. [[CrossRef](#)] [[PubMed](#)]